16. Jones GB, Midgley RL, Smith GS. Massive osteolysis. Disappearing bones. *J Bone Joint Surg (Br)* 1958;403:494-496.
17. Sty JR, Thomas JP, Wolff MH, Litwin SB Lymphoscintigraphy. Pulmonary lymphangiectasia. *Clin Nucl Med* 1984;9:716.
18. Goens MB, Campbell D, Wiggins JW. Spontaneous chylothorax in Noonan syndrome. Treatment with prednisone. *Am J Dis Child* 1992;146:1453-1456.
19. Donnenfeld AE, Nazir MA, Sindoni F, Librizzi RJ. Prenatal sonographic documentation of cystic hygroma regression in Noonan syndrome. *Am J Med Genet* 1991;39: 461-465.
20. Nistal M, Paniagua R, Bravo MP. Testicular lymphangiectasis in Noonan's syndrome. *J Urol* 1984;131:759-761.
21. Vallet HL, Holtzapple PG, Ebeerlein WR, Yakovac WC, Moshang T, Bongiovanni AM. Noonan syndrome with intestinal lymphangiectasis. A metabolic and anatomic study. *J Pediatr* 1972;80:269-274.
22. White SW. Lymphedema in Noonan's syndrome. *Int J Dermatol* 1984;23:656-657.
23. Hoeffel JC, Juncker P, Remy J. Lymphatic vessels dysplasia in Noonan's syndrome. *AJR* 1980;134:399-401.
24. Minkin W, Frank SB, Wolman SR, Cohen HJ. Lymphedema in Noonan's syndrome. *Int J Dermatol* 1974;13:179-183.
25. Herzog DB, Logan R, Kooistra JB. The Noonan syndrome with intestinal lymphangiectasia. *J Pediatr* 1976;88:270-272.
26. Mendez HM, Opitz JM. Noonan syndrome: a review. *Am J Med Gen* 1985;21:493-506.
27. Gloviczki P. Lymphatic reconstructions. In: Rutherford RB, ed. *Vascular surgery*, 4th ed. Philadelphia: WB Saunders; 1995:1936-1950.
28. Gloviczki P, Wahner HW. Clinical diagnosis and evaluation of lymphedema. In: Rutherford RB, ed. *Vascular surgery*, 4th ed. Philadelphia: WB Saunders; 1995:1899-1920.

Rat Antigen-Induced Arthritis: Cartilage Alterations Assessed with Iodine-123-Antileukoproteinase

Raimund W. Kinne, Philipp Meyer, Winfried Gründer, Eberhard Buchner, Ernesta Palombo-Kinne, Regina Heinzel-Wieland, Wolfgang Becker, Friedrich Wolf, Joachim R. Kalden and Harald Burkhardt

Institute of Clinical Immunology and Transfusion Medicine and Institute of Biophysics, University of Leipzig, Leipzig, Germany; Fachbereich Chemische Technologie, Fachhochschule Darmstadt, Darmstadt, Germany; and Department of Nuclear Medicine and Institute of Clinical Immunology and Rheumatology, Department of Internal Medicine III, University of Erlangen-Nuremberg, Nuremberg, Germany

Imaging of cartilage alterations was attempted in joints of rats with chronic antigen-induced arthritis (AIA) using the cationic ^{123}I-labeled serine proteinase inhibitor antileukoproteinase (^{123}I-ALP; pI > 10), which selectively accumulates in normal cartilage, presumably through interaction with negatively charged proteoglycans. **Methods:** Iodine-123-ALP or ^{123}I-myoglobin, a control protein of comparable size but with different isoelectric point (pI = 7.3) was injected intravenously into normal or AIA rats. Joint accumulation was followed by scintigraphy for 14 hr. Tissue radioactivity was assessed by well-counter measurements after dissection. The content of charged molecules in articular cartilage was determined by toluidine blue staining; the degree of joint destruction was assessed in parallel by x-ray, ex vivo MRI and histopathology. **Results:** In intact articular cartilage, ALP accumulated to a significantly higher degree than myoglobin. This preferential accumulation was lost in rats with chronic AIA. The target-to-background ratio for ^{123}I-ALP negatively correlated with the loss of toluidine blue staining in cartilage, which documents depletion of charged matrix molecules ($r = -0.92$, $p < 0.01$ at 4 hr; $r = -0.97$, $p < 0.01$ at 13 hr). ALP scintigraphy was sensitive in detecting cartilage alterations, even though the degree of joint destruction and inflammatory infiltration was mild, as demonstrated by x-ray, MRI and histopathology. **Conclusion:** In rat AIA, loss of ALP accumulation appears to document proteoglycan depletion in mildly altered arthritic cartilage. ALP scintigraphy may represent a functional assay for early, premorphological cartilage alterations in human arthritis as well.

Key Words: scintigraphy; x-ray; MRI; iodine-123; antileukoproteinase

J Nucl Med 1998; 39:1638-1645

Proteolytic degradation of proteoglycans and collagens in cartilage matrix is a common feature of degenerative and chronic inflammatory joint diseases (*1*). In these disorders a disturbance of the balance between tissue-degrading enzymes, such as metallo- and serine proteinases, and their inhibitors may contribute to increased cartilage matrix catabolism (*2,3*).

Recently, an 11-kDa serine proteinase inhibitor was isolated from human articular cartilage (*4*) and identified as antileukoproteinase (ALP) (5). Interestingly, ALP expression in resident joint cells is below the detection limit of immunohistology and in situ hybridization (*6*), and no unequivocal ALP synthesis by chondrocytes can be demonstrated after biosynthetic labeling in vitro. It is, therefore, likely that ALP is produced at extra-articular sites such as the mucosa of bronchi and urogenital tract, as well as salivary and lacrimal glands (*7–10*), from which it is transferred into synovial fluid through the circulation (*11*). Indeed, the cationic molecule ALP (pI > 10) selectively accumulates in the joints of normal animals (*12*). Within individual joint structures, this accumulation is highly selective for articular cartilage, as shown by immunoprecipitation assays (*12*). Such entrapment most likely results from charge interactions with negatively charged proteoglycans.

Thus, serum-derived inhibitor molecules such as ALP, which physiologically accumulate in normal cartilage, can be exploited as targeting molecules for scintigraphic revelation of biochemical alterations in arthritic cartilage, for example, the loss of proteoglycans (*13*). This is of particular interest in view of the fact that conventional imaging techniques used in clinical routine, such as radiography or even MRI, document morphological abnormalities of cartilage only at stages in which damage is already fairly advanced and mostly irreversible (*14–16*).

Therefore, ^{123}I-labeled serine proteinase inhibitor ALP (^{123}I-ALP) was injected intravenously into rats with experimental antigen-induced arthritis (AIA). Its accumulation in cartilage was monitored by gamma camera imaging and well-counter measurements of tissue specimens. AIA was chosen because it is a chronic model of arthritis characterized by relatively slow joint destruction and low-grade chronic inflammation (*17*). This minimizes the influence of nonspecific accumulation of proteins due to increased endothelial permeability.

Received Jun. 18, 1997; revision accepted Dec. 3, 1997.
For correspondence or reprints contact: Raimund W. Kinne, MD, Experimental Rheumatology Unit, Bachstr. 18, D-07740 Jena, Germany.

MATERIALS AND METHODS

Animals

Female inbred Lewis rats (Charles River, Sulzfeld, Germany; age range 6–8 wk; body weight 150–170 g) were housed in cages under standard animal room conditions. One to 2 wk after arrival were allowed for acclimatization. At the time of scintigraphy, the rats weighed between 181 and 250 g.

Induction of Antigen-Induced Arthritis

Antigen-induced arthritis was induced as described previously (*17*). Briefly, rats were immunized subcutaneously twice (21 and 14 days before AIA induction) with a suspension of 1 ml methylated bovine serum albumin (mBSA) in phosphate-buffered saline (PBS) (500 μg/ml mBSA in PBS; Sigma, Deisenhofen, Germany) and 1 ml of Freund's complete adjuvant (FCA) [2 mg/ml *Mycobacterium tuberculosis* H37 Ra in Freund's incomplete adjuvant (FIA); both from Difco, Augsburg, Germany]. On Day 0, a monoarticular arthritis was induced by intra-articular injection of 500 μg mBSA in 50 μl PBS into the right knee joint. The left knee was injected with PBS only and served as reference for the measurement of joint swelling.

Clinical Assessment of Arthritis

The size of the knee joints was determined by measuring the medial-lateral diameter with a caliper before and at regular intervals after induction of arthritis. Swelling was expressed as the difference in millimeters between the diameter of the arthritic (right) and that of the reference (left) knee.

The increased uptake of ^{99m}Tc-pertechnetate ($^{99m}TcO_4$) in arthritic knee joints, an objective parameter to measure articular inflammation (reference 22 in *12*), also was assessed. Briefly, 37 MBq $^{99m}TcO_4$ in 0.5 ml 0.9% NaCl were injected intraperitoneally under chloralhydrate-induced anesthesia (10 ml of a 2.25% solution/kg body weight, intraperitoneally); 30–40 min thereafter, the joint uptake of the radioactive compound was determined using a gamma camera (Basicam) equipped with a high-resolution pinhole collimator (both from Siemens, Erlangen, Germany). The levels of radioactivity contained in both knee joints were quantified by means of the regions of interest (ROIs) technique. The data were expressed as the ratio between radioactivity levels in the arthritic (right) and the reference knee joint (left).

Radiographic/MRI Assessment of Joint Destruction and Cartilage Alterations

The severity of joint damage, in other words the degree of destruction of cortical bone and the formation of osteophytes, was assessed radiographically. A reliable evaluation of the narrowing of the joint space, as a direct measure of cartilage damage, was impossible due to the small size of the joints and the availability of one-view images only. Therefore, to unequivocally analyze cartilage alterations, in a separate group of AIA rats (n = 4), as well as in two normal animals, high-resolution MRI images were acquired on a BRUKER AMX 300 spectrometer (field strength 7.1 T) equipped with a microimaging unit. Spin-echo techniques were used (echo times 11 and 16 msec, and repetition times 500 and 1000 msec) to image the excised rat knees ex vivo. A matrix of 512 × 512 pixels was applied, yielding in-plane pixel resolution of 19 μm at a slice thickness of 500 μm. The acquisition times were 8–134 min.

Histopathological Assessment of Cartilage Alterations, Joint Destruction and Inflammatory Infiltration

After the animals were killed, both knee joints were excised, and skin and superficial muscles were removed. The samples were frozen in methylbutane cooled in liquid nitrogen and embedded in 8% gelatin. Cryosectioning of undecalcified joint samples was performed as described previously (reference 23 in *12*). Serial 8-μm-thick sections were attached to adhesive tape and stained with a 0.5% solution of toluidine blue at pH 5 for exactly 30 sec or, alternatively, with Giemsa solution (reference 24 in *12*). Sections were photographed using a Zeiss Axiophot microscope (Zeiss, Jena, Germany).

TABLE 1
Histopathological Evaluation of the Severity of Antigen-Induced Arthritis (AIA)

	Normal (n = 12)	AIA (n = 12)
Loss of toluidine blue staining (proteoglycan depletion)	0.00 ± 0.00	0.96 ± 0.15*
Joint destruction	0.00 ± 0.00	1.00 ± 0.16*
Inflammatory infiltration	0.00 ± 0.00	1.47 ± 0.16*

Loss of toluidine blue staining and degree of inflammatory infiltration (mean ± s.e.m.) were evaluated using a semiquantitative score in which 1 = mild, 2 = moderate and 3 = severe alterations; joint destruction was semiquantified with a score from 0 to 4 (for details, see Materials and Methods section).

*$p \leq 0.0001$ for the comparison between AIA and normal controls.

The loss of toluidine blue staining in the cartilage (representing the loss of charged molecules) and the degree of inflammatory infiltration and joint destruction in arthritic joints were assessed in a blinded fashion by two independent observers using a semiquantitative score in which 1 = mild, 2 = moderate and 3 = severe alterations. In the case of toluidine blue staining, the evaluation was based on the intensity of cartilage coloring, as well as on the degree of destaining within the matrix or around the chondrocytes. Because the cartilage of normal rats did not always show maximal staining (depletion score 0.25 ± 0.03; n = 12), this score was subtracted from the values of both normal and arthritic rats to assign a value of 0 to the loss of proteoglycan in normal rats (Table 1).

The inflammatory infiltration was quantified on the basis of the relative number and density of infiltrating leukocytes in the synovial membrane.

Joint destruction was graded as 1 = unequivocal erosion of <10% of cartilage and bone cross-sections, 2 = erosion of 10%–25%, 3 = erosion of 25%–50%, and 4 = erosion of >50% of cartilage and bone cross-sections.

Radiolabeling of Antileukoproteinase and Myoglobin

Recombinant ALP (11 kDa, pI > 10) and myoglobin (17 kDa, pI = 7.3; Sigma) were radiolabeled with ^{123}I by the iodogen method (reference 25 in *12*) and, before their use in animal experiments, separated from unbound iodine by size-exclusion chromatography on Sephadex G-25 columns (PD-10; Pharmacia Biotech, Freiburg, Germany).

Quality Control of the Radiopharmaceuticals

The percentage of protein-bound or free iodine was determined within 1 hr following labeling by size chromatography of the injectants over PD-10 columns (Pharmacia Biotech).

Plasma Clearance of Antileukoproteinase

Clearance of ALP from circulation was determined by well-counter measurements of radioactivity contained in arterial plasma aliquots of one arthritic rat 1, 2, 4, 6, 10 and 17 hr following central intravenous injection. In addition, sodium dodecyl sulfate polyacrylamide gel electrophoresis (SDS-PAGE; 8%–18% polyacrylamide) of the plasma samples was performed to determine the size of the protein carrying the radioisotope; the radioactivity contained in the band corresponding to ALP was determined by autoradiography and quantified using an image analysis system (Cybertech, Berlin, Germany).

TABLE 2
Distribution of Radioactivity in Plasma and Individual Tissues of the Joint Region

Tissue	Myoglobin		ALP	
	Normal (n = 5)	AIA (n = 6)	Normal (n = 7)	AIA (n = 6)
Tibia cartilage	0.22 ± 0.04	0.16 ± 0.03	0.58 ± 0.14*	0.14 ± 0.03†
Femur bone	0.07 ± 0.01	0.05 ± 0.00	0.09 ± 0.02	0.06 ± 0.01
Bone marrow	0.07 ± 0.01	0.05 ± 0.01	0.03 ± 0.00*	0.04 ± 0.02
Synovia	0.24 ± 0.03	0.62 ± 0.17†	0.18 ± 0.04	0.15 ± 0.02*
Skeletal muscle	0.07 ± 0.02	0.04 ± 0.00	0.05 ± 0.01	0.03 ± 0.00†
Skin	0.19 ± 0.03	0.18 ± 0.02	0.28 ± 0.04	0.19 ± 0.04
Plasma	2.05 ± 0.31	1.32 ± 0.13	0.64 ± 0.09*	0.44 ± 0.09*

*$p \leq 0.05$ for the comparison between ALP and myoglobin.
†$p \leq 0.05$ for the comparison between AIA and normal rats.
Mean ± s.e.m. of the % injected activity per g sample wet weight. AIA = antigen-induced arthritis; ALP = antileukoproteinase.

Intravenous Injection and Imaging

For intravenous delivery of the injectants, a 7-cm-long polyethylene catheter (Bardi-Kath; Bard Limited, Sunderland, United Kingdom) was inserted into the right common jugular vein under anesthesia with diethyl-ether (Merck, Darmstadt, Germany). The opposite end of the catheter, covered with a rubber head, was subcutaneously led to emerge from the dorsal neck and sutured below the interauricular line. For sampling of arterial blood, the same technique was used to catheterize the right carotid artery. After recovery for at least 2 hr, the rats were anesthetized again by intramuscular injection of urethane (0.75 g/kg body weight; Sigma) and immobilized on a stretcher beneath a gamma camera. Three hundred micrograms (~55 MBq) ^{123}I-ALP or equimolar amounts of the control protein were injected slowly through the central venous catheter. The accumulation radiolabeled ALP (n = 4 normals; n = 6 AIA) or myoglobin (n = 3 normals; n = 6 AIA) in knee and ankle joints was followed in 15-min frames for 14 hr using a Siemens Basicam gamma camera, equipped with a pinhole collimator and interfaced to a Micro-Delta computer system (all Siemens). Integrated radioactivity distribution was measured using a 128 × 128 matrix.

Evaluation of Scans

Pinhole images of arthritic and normal recipient rats were evaluated using the ROI technique. Regions of interest were placed over the right knee and ankle joints. Reference regions of equal size were placed over the proximal or distal lower legs, respectively, immediately adjacent to the ROIs. The results were expressed as counts accumulated in the two regions during time frames of 15 min, corrected for the decay of ^{123}I. For determination of the target-to-background (T/B) ratio, the data were expressed as the ratio between radioactivity levels in the knee or ankle joint region, and those in the lower leg used as reference regions (*18,19*).

Biodistribution of Antileukoproteinase and Myoglobin

Seventeen hours after injection, the tissues listed in Table 2 were excised after withdrawal of 7–8 ml of blood by heart puncture. Sampling was performed, as described previously (*18*), with minor modifications. The radioactivity contained in the different preparations after injection of radiolabeled ALP (n = 7 normals; n = 6 AIA) or myoglobin (n = 5 normals; n = 6 AIA) was counted in a gamma well counter. Values were expressed as percentage of injected activity/gram of wet weight of the samples.

Statistical Analysis

Differences in the ROI evaluation and in the accumulation of ALP or myoglobin in different tissues, as well as in the histopathological parameters, were analyzed by means of the Mann–Whitney U-test. Correlations between different parameters were examined by means of Spearman rank correlation. Analyses were performed using the StatView 4.0 program. In all cases significant differences were accepted for $p \leq 0.05$.

RESULTS

Clinical and Histopathological Evaluation of Antigen-Induced Arthritis

Clinical Assessment. After an ~1-wk-long acute phase, the monoarticular knee arthritis decreased within 2 wk to a low-grade, chronic swelling. The rats were used 80 ± 3 days after induction of AIA, i.e., 2.5 mo into the chronic phase of the disease.

The maximal joint swelling during the acute phase was similar in the ALP-injected group (2.2 ± 0.2 mm; mean ± s.e.m.; n = 6) and the myoglobin-injected group (2.3 ± 0.2 mm; n = 6). At the time of scintigraphy (day 80 ± 3), however, the joint swelling was 0.3 ± 0.2 mm in the ALP-injected group and 0.8 ± 0.1 mm in the myoglobin-injected group; although the swelling was significantly (and unexpectedly) higher in the latter group ($p = 0.04$), the uptake of $^{99m}TcO_4$ did not significantly differ between the two groups (arthritic-to-reference joint ratio: ALP, 1.1 ± 0.0; myoglobin, 1.1 ± 0.0). Indeed, there was no significant correlation between $^{99m}TcO_4$ uptake and clinical scores of individual animals (data not shown). In the chronic phase of disease, thus, the $^{99m}TcO_4$ uptake may not be particularly sensitive in detecting modest clinical differences.

Radiographic/MRI Assessment of Joint Destruction and Cartilage Alterations. Although direct signs of cartilage alterations in the AIA knee joints (i.e., narrowing of the joint space) could not be unequivocally detected by radiography, mild cartilage alterations could be indirectly documented by the presence of bone erosions and osteophytes (score 1.1 ± 0.2; mean ± s.e.m.; n = 12).

High-resolution MRI analysis revealed only a limited degree of cartilage alterations in a separate group of four AIA rats with a mild degree of arthritis (Fig. 1, B and D; joint swelling 0.7 ± 0.5; mean ± s.e.m.), when compared to two normal rats (Fig. 1, A and C).

Histopathological Assessment of Cartilage Alterations, Joint Destruction and Inflammatory Infiltration. There was depletion of charged molecules in the cartilage of AIA rats, as reflected by the loss of toluidine blue staining in comparison with normal cartilage (Table 1; Fig. 2). On average, however, the degree of the loss of staining in AIA cartilage was fairly mild (score of ~1 on a scale of 1–3; Table 1). The extent of joint destruction also was mild (score of ~1, i.e., erosion of <10% of cartilage

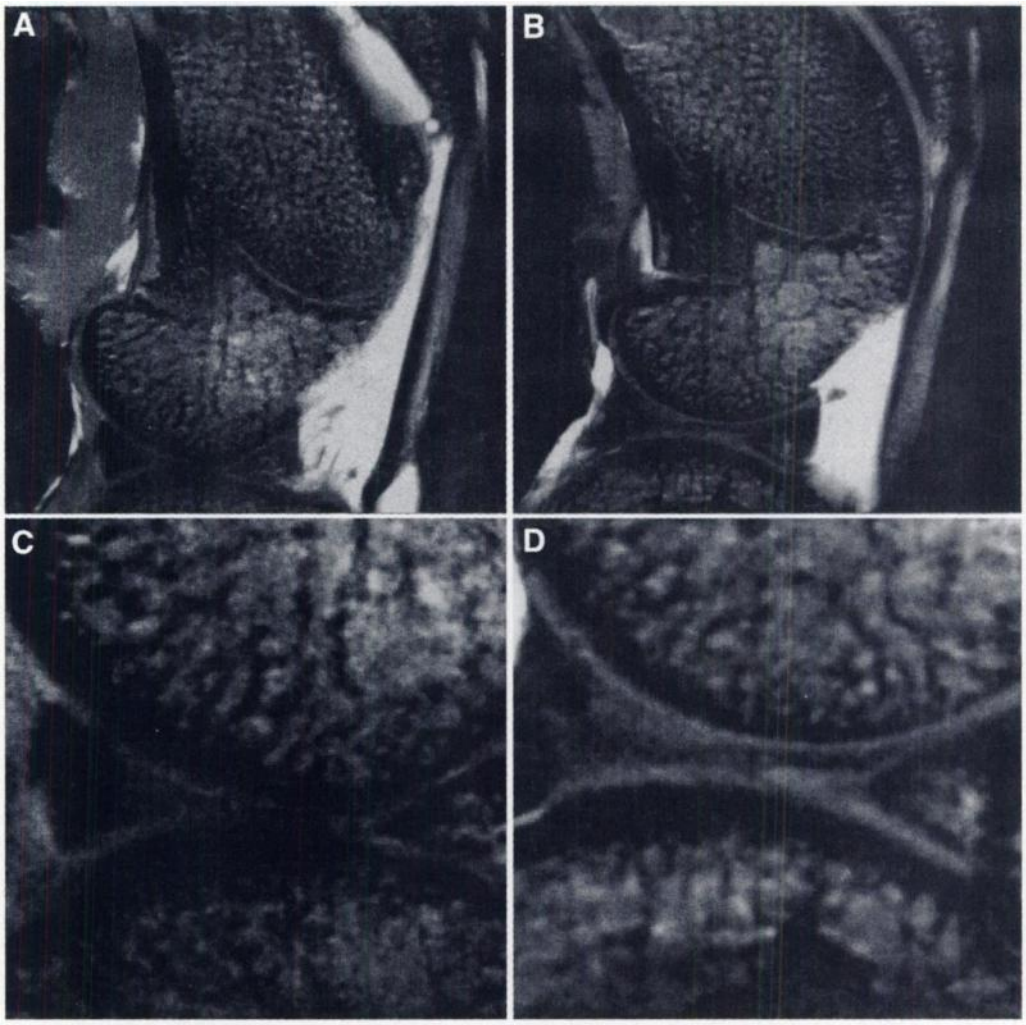

FIGURE 1. Ex vivo high-resolution MRI images (A and B; magnifications in C and D, respectively) of knee joints from normal (A and C) and AIA rats (B and D). AIA rats did not show clear morphological signs of cartilage alteration, with the possible exception of two small defects (upper left quadrant in D) exclusively observed in the rat with the highest concomitant joint swelling (2.1 mm) among the four animals investigated (0.0, 0.3, 2.1 and 0.3 mm; mean ± s.e.m. 0.7 ± 0.5 mm).

and bone cross-sections), and that of chronic inflammatory infiltration was mild to moderate (score of ~1.5; Table 1).

Scintigraphic Evaluation of Cartilage Alterations in Antigen-Induced Arthritis

Quality Control of the Radiopharmaceuticals. Iodine-123-ALP (Fig. 3A) and myoglobin (Fig. 3B) contained more than 90% and more than 81% of the injected activity, respectively, in protein-bound form. The remaining activity eluted in a broad peak corresponding to the profile of free iodine (Fig. 3C).

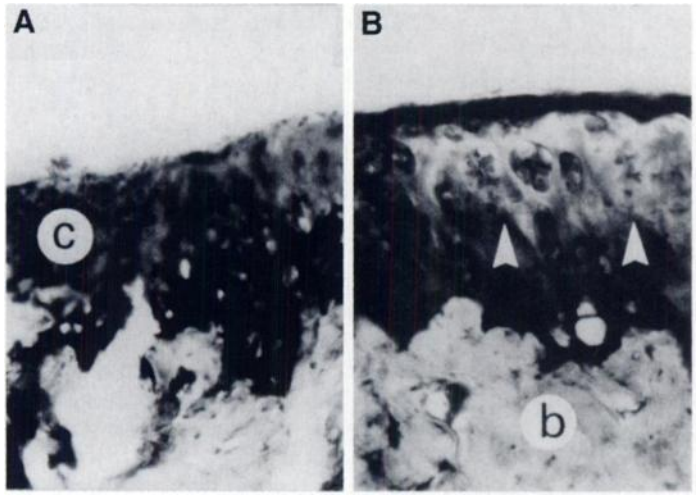

FIGURE 2. Toluidine blue staining of (A) normal and (B) arthritic cartilage. The decrease of the staining in arthritic cartilage (arrowheads in B) most likely reflects the loss of charged proteoglycans from the cartilage matrix; c = cartilage; b = bone. For reasons of clarity, an animal with more marked alterations (score 2) than the mean value (score of ~1; Table 1) is shown. Original magnification, ×186.

Plasma Clearance of Antileukoproteinase. Plasma levels of ALP decreased from 1.4% injected activity/gram plasma wet weight at 1 hr, over 1.1% at 2 hr and 1% at 4 hr, to 0.4% at 17 hr (Fig. 4A). The plasma $T_{1/2}$ was 0.5 hr between 1 and 2 hr, and 6.5 hr between 4 and 17 hr (Fig. 4A). The decrease of radioactivity in the ALP band, as detected by SDS-PAGE (Fig. 4B; $T_{1/2}$ = 6.5 hr), closely matched the findings obtained with direct plasma radioactivity measurements between 4 and 17 hr (Fig. 4, A and B).

Joint Accumulation of Antileukoproteinase. There was preferential accumulation of ALP in normal knee joints in comparison with myoglobin (Fig. 5, A and B). Quantitation of the radioactivity levels in knee joint and reference region confirmed higher joint values (Fig. 6, A and B) and significantly higher T/B ratios for ALP than for myoglobin (1.25-fold at 11.5 hr; $p \leq 0.05$ from 2.75 to 12 hr; Fig. 6, C and D).

The selective accumulation of ALP in normal knee joints was lost in the arthritic knees of AIA rats (Fig. 5, D and E, and Fig. 6, A and B). For ALP, the T/B ratio between ROI and reference region was no longer significantly different from myoglobin, if it was at all numerically lower (Fig. 6, C and D). In contrast, the ankle joints of AIA rats (i.e., the joint presumably not affected by the arthritic process) remained capable of specifically accumulating ALP (Fig. 6, E and F; $p \leq 0.05$ from 3 to 12.25 hr in comparison with myoglobin; n = 6 rats).

Of note, the T/B ratio observed with ALP scintigraphy but

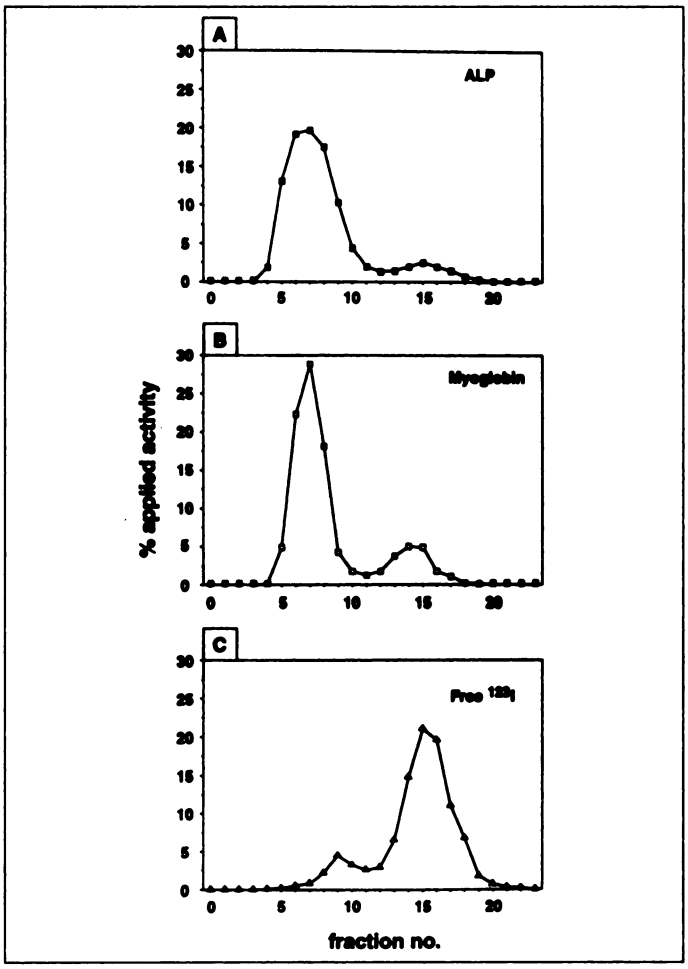

FIGURE 3. Size chromatography of (A) ^{123}I-ALP, (B) ^{123}I-myoglobin and (C) free iodine on PD-10 columns within 1 hr following radiolabeling. Radiopharmaceuticals were eluted in 250-μl fractions. ALP contained ~10% free iodine, and myoglobin contained ~19% free iodine.

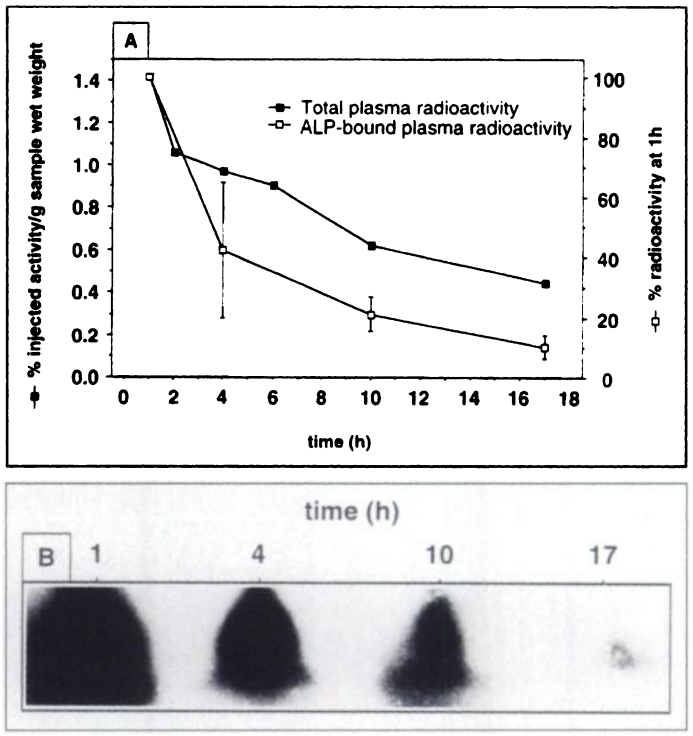

FIGURE 4. Plasma clearance of ^{123}I-ALP in one arthritic animal. (A) The $T_{1/2}$ was 0.5 hr between 1 and 2 hr, and 6.5 hr between 4 and 17 hr. (B) The decrease of ALP activity in SDS-PAGE paralleled the decrease seen in the plasma between 4 and 17 hr ($T_{1/2}$ was also 6.5 hr).

not that seen with myoglobin showed a highly significant, negative correlation with the degree of loss of toluidine blue staining in the cartilage of excised knee joint samples ($r = -0.92$, $p < 0.01$ at 4 hr, Fig. 7A; $r = -0.97$, $p < 0.01$ at 13 hr; all other time points, $r \leq -0.71$, $p \leq 0.05$, $n = 10$ from 1 hr to 10.5 hr, and $n = 9$ from 11 to 13.5 hr).

Distribution of Radioactivity Within Individual Joint Structures. For more detailed analysis of individual structures of the joint region, the animals were dissected and the tissue radioactivity was measured directly. In normal tibia cartilage, ALP accumulated to a significantly higher degree than myoglobin (Fig. 8). In contrast, in AIA animals, ALP accumulated in the cartilage to the same extent as myoglobin (Fig. 8). As already observed for the T/B ratio in ALP scintigraphy, there was a significant, negative correlation between the specific accumulation of ALP in cartilage and the degree of loss of toluidine blue staining in the cartilage of excised knee joint samples ($r = -0.79$; $p < 0.05$; $n = 10$; Fig. 7B).

Unlike ALP, myoglobin accumulated to a significantly higher degree in normal bone marrow (Fig. 8), a joint structure known to be highly perfused. In addition, the inflamed synovial membrane of AIA rats showed a significantly higher accumulation of myoglobin than ALP (Fig. 8), a finding compatible with increased permeability of inflamed tissues for proteins. In individual rats, indeed, there was a significant correlation between the myglobin accumulation in the inflamed synovial membrane and the degree of joint swelling on one hand ($r = 0.92$; $p < 0.01$; $n = 10$) and the degree of inflammatory infiltration on the other hand ($r = 0.69$; $p = 0.02$; $n = 11$). Because the inflamed synovial membrane shows high endothelial permeability and vascularization, and inasmuch as myoglobin maintains high plasma levels throughout scintigraphy (Table 2), myoglobin thus may be particularly suitable to depict residual inflammation (Fig. 8). On the other hand, the apparent failure of ALP to accumulate in the AIA synovial membrane (Table 2) is most likely due to the low inflammation scores of the respective group.

Distribution of Radioactivity in Extra-articular Tissues. The plasma values of myoglobin remained significantly higher than those of ALP in both normal and AIA rats (Table 2). Notably, the levels of ALP in skeletal muscle of arthritic animals were significantly lower than in normals (Table 2), possibly in relationship to secondary muscle hypotrophy.

DISCUSSION

These results demonstrate, both qualitatively (Fig. 5) and quantitatively (Fig. 6), that radiolabeled ALP accumulates to a higher degree than myoglobin, a control protein of similar size but with a different isoelectric point, in the joints of normal rats. The direct measurement of radioactivity in different joint tissues (Fig. 8) supports immunoprecipitation results showing that the ALP accumulation is confined to the cartilage matrix (*12*). Although it is remarkable that such clear joint accumulation of ALP can be achieved at all on systemic injection, it is consistent with the physiological distribution of ALP through the bloodstream (*11*) and the synovial fluid (*5*).

In contrast to ALP, myoglobin does not exhibit an affinity for cartilage (whether normal or diseased) but, rather, accumulates in highly perfused compartments of the joint, such as the inflamed synovial membrane or the bone marrow adjacent to the cartilage (Fig. 8; Table 2), consistently also with the high plasma levels of myoglobin (Table 2) (*20,21*). In contrast to

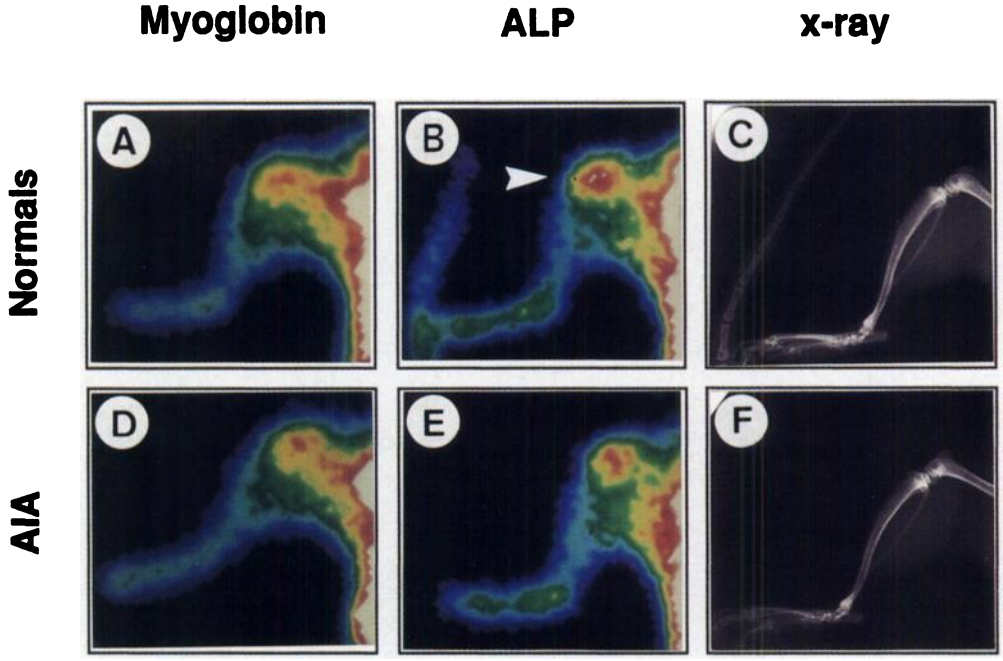

FIGURE 5. (A, B, D, E) Gamma camera and (C and F) x-ray images of representative (A–C) normal and (D–F) arthritic rats ~6 hr after intravenous injection of (B and E) ^{123}I-ALP or (A and D) the control protein ^{123}I-myoglobin. Colors range from blue (low radioactivity) to white (high radioactivity). In normal knee joints, both injectants clearly accumulated in the (A and B) central region of the joint, with higher accumulation of (arrowhead in B) ALP. In arthritic joints, in contrast, the visual difference between (E) ALP and (D) myoglobin was lost.

myoglobin, ALP showed low plasma levels throughout the study (Table 2). Although this could be due to extraction of ALP from circulation by cartilagenous tissues, both in the joints (Table 2; Fig. 8) and at extra-articular locations (*12*), on the other hand the cartilage uptake is relatively low (0.58% injected activity/gram; Table 2) and the total cartilage mass in the body

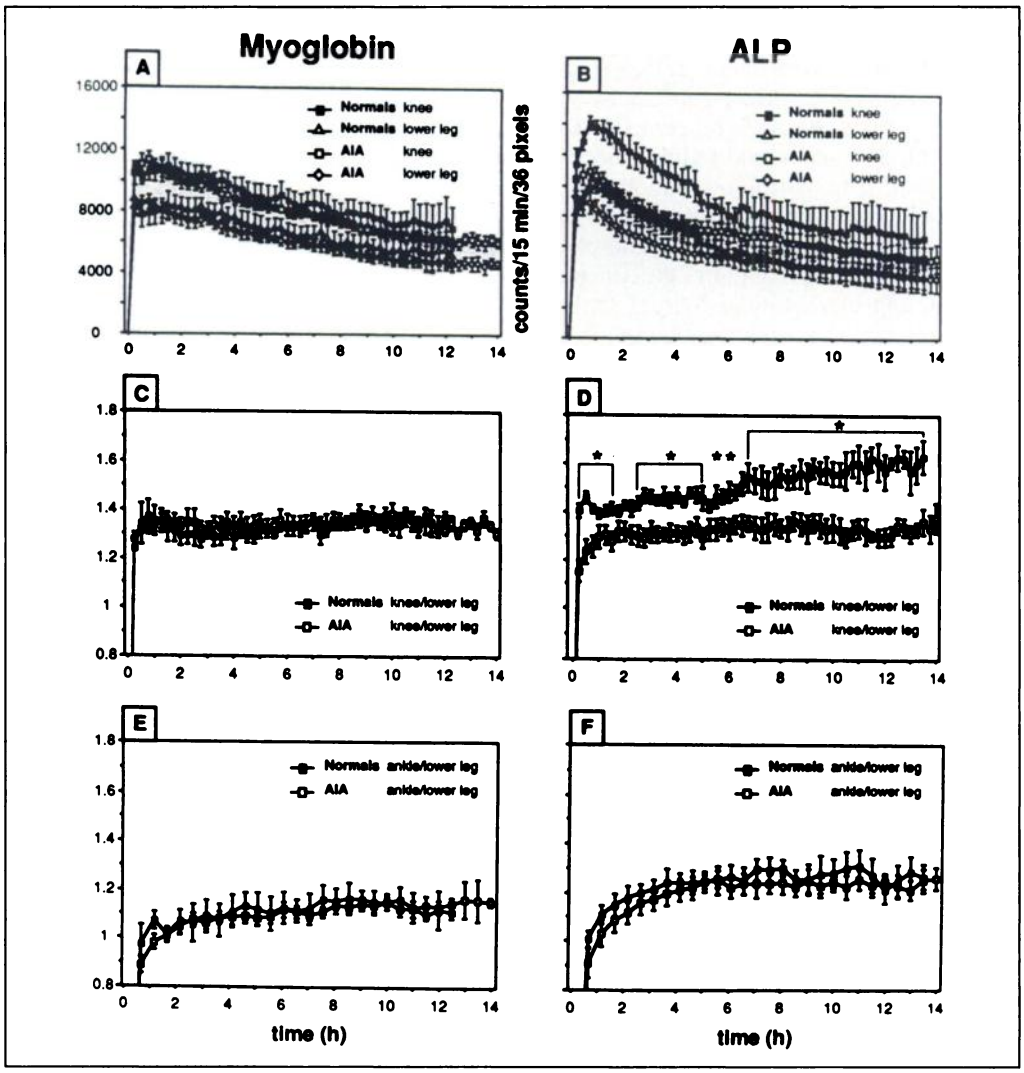

FIGURE 6. Joint uptake in (A–D) normal and arthritic knees, as well as in (E and F) ankle joints (with proximal and distal lower leg as respective reference regions) after intravenous injection of (A, C, E) ^{123}I-myoglobin or (B, D, F) ^{123}I-ALP (mean ± s.e.m.; $*p \leq 0.05$ for the comparison between normals and AIA). (B) The accumulation of ALP in normal knees and (D) the resulting T/B ratio were significantly higher than those of (A and C) myoglobin ($p \leq 0.05$ from 2.75 to 12 hr). This difference was lost in (A–D) AIA knee joints. In contrast, in the ankle joint of AIA rats (i.e., a joint most likely excluded from the arthritic process), the (F) ALP accumulation was largely retained in comparison with that of (E) myoglobin ($p \leq 0.05$ from 3–12.25 hr).

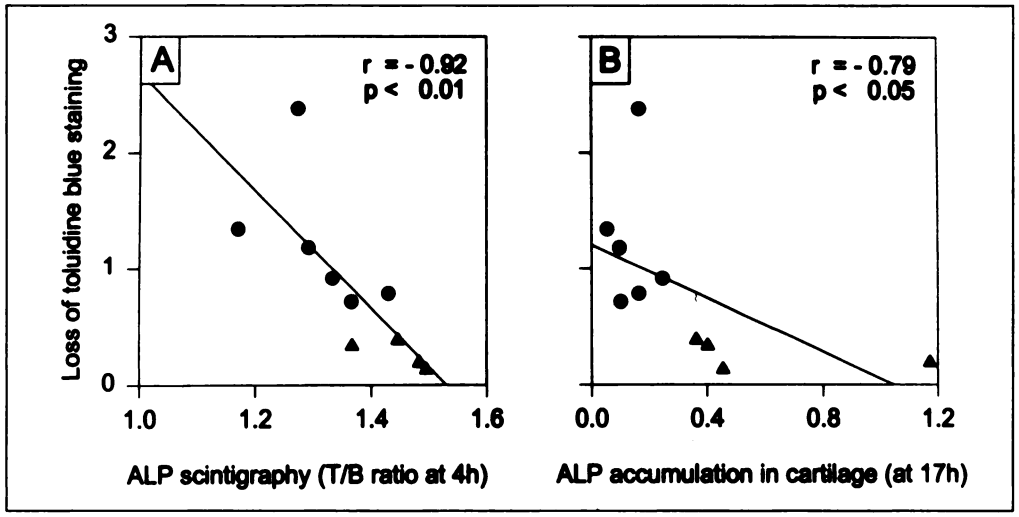

FIGURE 7. Spearman rank correlation between the loss of toluidine blue staining (which reflects the loss of negatively charged proteoglycans) and (A) the T/B ratio obtained on ^{123}I-ALP scintigraphy or (B) direct measurements of radioactivity in excised cartilage after completion of ^{123}I-ALP scintigraphy in AIA rats (n = 6; circles) and normal rats (n = 4; triangles).

is fairly limited. Other, noncharacterized mechanisms are, therefore, likely to contribute to this phenomenon.

The specific accumulation of ALP was lost in the cartilage of AIA rats (this study) (*12*). This is most likely due to the loss of negatively charged proteoglycans (Table 1; Fig. 2), such as aggrecan, or the small proteoglycans biglycan, fibromodulin and decorin (*22*), to which the highly cationic proteinase inhibitor ALP attaches through charge interactions (*23*). This hypothesis is supported by significant correlations between the loss of toluidine blue staining in arthritic cartilage and the T/B ratio in ALP scintigraphy as well as between the loss of toluidine blue staining in arthritic cartilage and the accumulation of ALP in excised tibia cartilage (Fig. 7).

In the AIA model, ALP scintigraphy was very sensitive in detecting limited degrees of proteoglycan depletion in the cartilage of chronically and mildly affected joints. In contrast, conventional radiological evaluation of cartilage damage in human and experimental arthritis attains diagnostic value only on narrowing of the joint space and/or appearance of bone erosions (*14–16*). At that point, the damage is fairly severe and advanced, and there remains only a limited time window for treatment aimed at preventing/slowing irreversible tissue damage. MRI, in turn, while strongly improving the visualization of morphological damage to the cartilage (*14*), remains of limited functional use on a single-patient basis because most significant differences are seen only in predefined groups of normal and osteoarthritis patients (*14*). The diagnostic potential of ALP scintigraphy, thus, being based on functional imaging with a molecule that selectively binds to components of the cartilage matrix and preceding morphological changes detectable by either x-ray or high-resolution MRI (Fig. 1) may be strongest in the period in which cartilage alterations are limited to fine biochemical changes (*24*). In addition to the diagnosis of early rheumatoid changes, ALP scintigraphy may, therefore, be useful for monitoring the effects of disease-modifying drugs, the efficacy of which, currently, can be proven only after long evaluation times by conventional radiography (*16*).

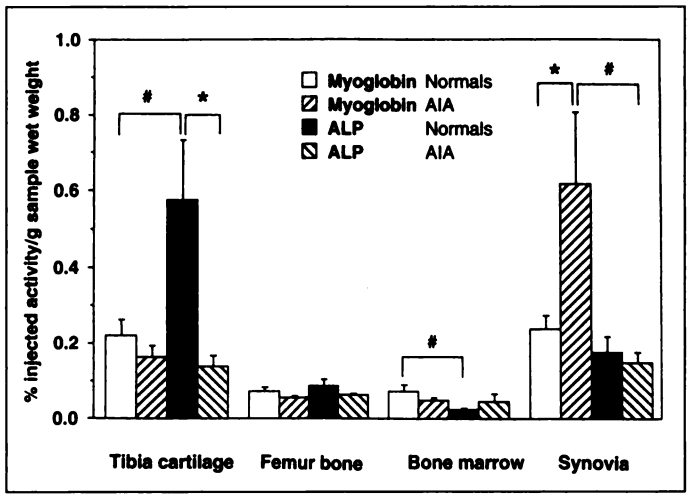

FIGURE 8. Tissue distribution 17 hr following intravenous injection of ^{123}I-ALP or ^{123}I-myoglobin into normal or arthritic rats (mean ± s.e.m. of percentage of injected radioactivity/g sample wet weight; n = 5–7 rats per group). However, ALP preferentially accumulates in normal tibia cartilage, myoglobin preferentially accumulates in highly perfused tissues such as bone marrow and arthritic knee synovia (see Table 2). *p ≤ 0.05 for the comparison between AIA and normals; #, p ≤ 0.05 for the comparison of ALP and myoglobin.

There have been several attempts to detect biochemical changes in the composition of articular cartilage in early stages of joint disease (*25–31*), for example, through measurement of cartilage metabolites in serum or synovial fluid. However, it is unclear whether these metabolites are formed during cartilage anabolism, turnover or catabolism (*25–28*), and, in addition, serum measurements do not allow monitoring of the degree of cartilage destruction in individual joints. More recently, potential markers of cartilage degradation, such as:

1. Structures at the nonreducing terminal of the chondroitin sulfate (CS) glycosamin side chains of proteoglycans,
2. Atypical sulfation patterns in native CS glycosaminoglycans of proteoglycans, and
3. A neoepitope created by cleavage of aggrecan by the matrix-metalloproteinase stromelysin,

have been targeted by means of specific antibodies (*29–31*). Although they successfully detect cartilage alterations in human rheumatoid arthritis (RA) and OA (*29*), as well as in stromelysin-injected rabbit joints (*30*) or experimental arthritis (*31*), the antibodies in some cases failed to reveal any changes, presumably because the target proteoglycan molecules were being excessively lost from the diseased tissue (*29*). The use of ALP scintigraphy, by depicting loss of cartilage proteoglycans rather than changes in their molecular structure, may, therefore, be more suitable for the diagnosis of arthritic/arthrotic cartilage alterations (*32*). In a Gd-conjugated form, ALP may be likewise suitable for high-resolution MRI (*33,34*).

The potential application of ALP scintigraphy in human cartilage/joint pathology requires several considerations. The identification of clinically unaffected joints that could serve as

reference ROIs may be difficult in the case of polyarticular arthritis. The use of external standards or joints that are characteristically (and/or relatively) spared in a particular disease could serve this purpose. In addition, there is the theoretical concern that the cold spot obtained with ALP imaging could be obscured by positive images based on the increased permeability for protein in the inflamed synovial membrane. Unlike in small rodents, however, the anatomical size of human joints may facilitate the discrimination of adjacent ROIs. Also, nonplanar methodologies (i.e., SPECT or PET) may be exploited to optimize the diagnostic potential of ALP scintigraphy.

CONCLUSION

ALP scintigraphy may represent a functional method for the detection of early cartilage alterations in arthritis/osteoarthritis, before irreversible cartilage damage takes place. This tool also may be useful to monitor the efficacy of treatments, whether surgical or pharmacological, aimed at preventing/reducing degeneration and injury of cartilage (*24*).

ACKNOWLEDGMENTS

This work was supported by the Wilhelm Sander Stiftung (grant 96.018.1 to H.B.) and by the German Ministry for Research and Technology (BMFT; grants FKZ 01VM8702 and 01VM9311). We thank Prof. K. von der Mark and Prof. F. Emmrich for financial support and B. Niescher and E. Bauer for excellent technical assistance. Recombinant antileukoproteinase was kindly provided by Grünenthal GmbH (Aachen, Germany).

REFERENCES

1. Werb Z, Alexander CM. Proteinases and matrix degradation. In: Kelley WN, Harris ED, Ruddy S, Sledge CB, eds. *Textbook of rheumatology*, 4th ed. Philadelphia, PA: WB Saunders Company; 1993:248–268.
2. Menninger H, Putzier R, Mohr W, Wessinghage D, Tillmann K. Granulocyte elastase at the site of cartilage erosion by rheumatoid synovial tissue. *Z Rheumatol* 1980;39: 145–156.
3. Vincenti MP, Clark IM, Brinckerhoff CE. Using inhibitors of metalloproteinases to treat arthritis: easier said than done? *Arthritis Rheum* 1994;37:1115–1126.
4. Burkhardt H, Kasten M, Rauls S. Purification and characterization of a serine proteinase inhibitor from human articular cartilage. *Biochim Biophys Acta* 1987;924: 312–318.
5. Böhm B, Deutzmann R, Burkhardt H. Purification of a serine-proteinase inhibitor from human articular cartilage: identity with the acid-stable proteinase inhibitor of mucous secretions. *Biochem J* 1991;274:269–273.
6. Böhm B, Aigner T, Kinne R, Burkhardt H. The serine-protease inhibitor of cartilage matrix is not a chondrocytic gene product. *Eur J Biochem* 1992;207:773–779.
7. Boudier C, Carvallo D, Bruch M, Roitsch C, Courtney M, Bieth JG. Human bronchial proteinase inhibitor: rapid purification procedure and inhibition of leukocyte elastase in presence and in absence of human lung elastin. *Adv Exp Med Biol* 1988;240:115–122.
8. Heinzel R, Appelhans H, Gassen G, et al. Molecular cloning and expression of cDNA for human antileukoprotease from cervix uterus. *Eur J Biochem* 1986;160:61–67.
9. Seemüller U, Arnhold M, Fritz H, et al. The acid-stable proteinase inhibitor of human mucous secretions (HUSI-I, antileukoprotease): complete amino acid sequence as revealed by protein and cDNA sequencing and structural homology to whey proteins and Red Sea turtle proteinase inhibitor. *FEBS Lett* 1986;199:43–48.
10. Thompson RC, Ohlsson K. Isolation, properties, and complete amino acid sequence of human secretory leukocyte protease inhibitor, a potent inhibitor of leukocyte elastase. *Proc Natl Acad Sci USA* 1986;83:6692–6696.
11. Fryksmark U, Ohlsson K, Rosengren M, Tegner H. A radioimmunoassay for measurement and characterization of human antileukoprotease in serum. *Hoppe-Seyler's Z Physiol Chem* 1981;362:1273–1277.
12. Burkhardt H, Meyer P, Buchner E, et al. The serine proteinase inhibitor antileukoproteinase specifically accumulates in normal but not in arthritic cartilage. *J Rheumatol* 1997;24:1145–1154.
13. Henderson B, Pettipher ER, Murphy G. Metalloproteinases and cartilage proteoglycan depletion in chronic arthritis: comparison of antigen-induced and polycation-induced arthritis. *Arthritis Rheum* 1990;33:241–246.
14. Kladny B, Swoboda B, Elbracht T, Willauschus W. Diagnosis of early stages of osteoarthritis in MRI. *Akt Rheumatol* 1996;21:17–20.
15. Blackburn WD, Bernreuther WK, Rominger M, Loose LL. Arthroscopic evaluation of knee articular cartilage: a comparison with plain radiographs and magnetic resonance imaging. *J Rheumatol* 1994;21:675–679.
16. Lohmander SL, Felson DT. Defining the role of molecular markers to monitor disease, intervention, and cartilage breakdown in osteoarthritis. *J Rheumatol* 1997;24:782–785.
17. Buchner E, Braeuer R, Emmrich F, Kinne RW. Induction of flare-up reactions in rat antigen-induced arthritis. *J Autoimmun* 1995;8:61–74.
18. Kinne RW, Becker W, Simon G, et al. Joint uptake and body distribution of a technetium-99m-labeled anti-rat-CD4 monoclonal antibody in rat adjuvant arthritis. *J Nucl Med* 1993;34:92–98.
19. Kinne RW, Becker W, Koscheck T, et al. Rat adjuvant arthritis: imaging with technetium-99m-anti-CD4 Fab' fragments. *J Nucl Med* 1995;36:2268–2275.
20. Gast A, Anderson W, Probst A, et al. Pharmacokinetics and distribution of recombinant secretory leukocyte proteinase inhibitor in rats. *Am Rev Respir Dis* 1990;141: 889–894.
21. Bergenfeldt M, Björk P, Ohlsson K. The elimination of secretory leukocyte protease inhibitor (SLPI) after intravenous injection in dog and man. *Scand J Clin Lab Invest* 1990;50:729–737.
22. Cs-Szabo G, Roughley PJ, Plaas AH, Glant TT. Large and small proteoglycans of osteoarthritic and rheumatoid articular cartilage. *Arthritis Rheum* 1995;38:660–668.
23. Van Lent PL, van den Berg WB, Schalkwijk J, van de Putte LB, van den Bersselaar L. The impact of protein size and charge on its retention in articular cartilage. *J Rheumatol* 1987;14:798–805.
24. Recht MP, Resnick D. Magnetic resonance imaging of articular cartilage: the state of the art. *J Rheumatol* 1995;22(suppl 43):52–55.
25. Manicourt DH, Fujimoto N, Obata K, Thonar EJ. Levels of circulating collagenase, stromelysin-1, and tissue inhibitor of matrix metalloproteinases 1 in patients with rheumatoid arthritis: relationship to serum levels of antigenic keratan sulfate and systemic parameters of inflammation. *Arthritis Rheum* 1995;38:1031–1039.
26. Manicourt DH, Fujimoto N, Obata K, Thonar EJ. Serum levels of collagenase, stromelysin-1, and TIMP-1: age- and sex-related differences in normal subjects and relationship to the extent of joint involvement and serum levels of antigenic keratan sulfate in patients with osteoarthritis. *Arthritis Rheum* 1994;37:1774–1783.
27. Mansson B, Carey D, Alini M, et al. Cartilage and bone metabolites in rheumatoid arthritis: differences between rapid and slow progression of disease identified by serum markers of cartilage metabolism. *J Clin Invest* 1995;95:1071–1077.
28. Lohmander LS. Markers of cartilage metabolism in arthrosis. *Acta Orthop Scand* 1991;62:623–632.
29. Slater RR, Bayliss MT, Lachiewicz PF, Visco DM, Caterson B. Monoclonal antibodies that detect biochemical markers of arthritis in humans. *Arthritis Rheum* 1995;38:655–659.
30. Bayne EK, MacNaul KL, Donatelli SA, et al. Use of an antibody against the matrix metalloproteinase-generated aggrecan neoepitope FVDIPEN-COOH to assess the effects of stromelysin in a rabbit model of cartilage degradation. *Arthritis Rheum* 1995;38:1400–1409.
31. Singer II, Kawka DW, Bayne EK, et al. VDIPEN, a metalloproteinase-generated neoepitope, is induced and immunolocalized in articular cartilage during inflammatory arthritis. *J Clin Invest* 1995;95:2178–2186.
32. Budinger TF, Taylor SE. New approaches to targeting arthritis with radiopharmaceuticals. *J Rheumatol* 1995;22(suppl 43):62–67.
33. Bradbeer JN, Kapadia RD, Sarkar SK, et al. Disease-modifying activity of SK&F 106615 in rat adjuvant-induced arthritis. *Arthritis Rheum* 1996;39:504–514.
34. Loeuille D, Gonord P, Guincamp C, et al. In vitro magnetic resonance microimaging of experimental osteoarthritis in the rat knee joint. *J Rheumatol* 1997;24:133–139.